$V_{\rm th}$ Model of Pocket-Implant MOSFETs for Circuit Simulation

D. Kitamaru, H. Ueno, K. Morikawa[1], M. Tanaka, M. Miura-Mattausch
H. J. Mattausch[1], S. Kumashiro[2], T. Yamaguchi[2], K. Yamashita[2], N. Nakayama[2]
Graduate School of Advanced Sciences of Matter,
[1]Research Center for Nanodevices and Systems,
Hiroshima University 1-4-1, Kagamiyama, Higashi-Hiroshima, 739-8527, Japan
Phone: +81-824-24-7637 Fax: +81-824-22-7195 E-mail: hq6@hiroshima-u.ac.jp
[2]Semiconductor Technology Academic Reserch Center,
3-17-2, Shin Yokohama, Kanagawa 222-0033

Abstract

A new threshold voltage ($V_{\rm th}$) model has been developed for the pocket-implant technology. The model extracts the threshold condition from the entire mobile charge concentration in the channel with only two parameters; the maximum doping concentration ($N_{\rm subp}$) of the pocket profile and the penetration length ($L_{\rm p}$) into the channel. The model reproduces the measured $V_{\rm th}$ *vs.* gate-length ($L_{\rm gate}$) characteristics with an average error of a few mV under any bias conditions.

1 Introduction

The pocket-implant technology enables $L_{\rm gate}$-reduction of MOSFETs down to the sub-$100nm$ region, because a strong reverse-short-channel effect (RSCE) suppresses the short-channel effect (SCE) on $V_{\rm th}$ [1]. However, the complicated $V_{\rm th}$-characteristic is not well understood and strongly dependent on the pocket-implant profile. This leads to 2 major concerns for practical applicability:

- a precise $V_{\rm th}$-model for circuit simulation, to enable correct design of analog and digital circuits
- an efficient method for pocket-implant optimization

Here we present a new $V_{\rm th}$-model, which is mainly targeted at resolving the circuit-simulation issue. In addition, the model can be used also for a first step optimization of the pocket profile.

2 Model description

Fig. 1 shows measured $V_{\rm th} - L_{\rm gate}$ characteristics. Specific feature is the strong RSCE suppressing SCE down to $L_{\rm gate} = 100nm$. To model this feature we determine $V_{\rm th}$ with the average carrier concentration ($n_{\rm av}$) along the channel, which is required to be equal to that at threshold condition ($n_{\rm th}$). Under the drift-diffusion approximation, the current density ($j_{\rm n}$) can be described by the gradient of the quasi-Fermi potential ($\phi_{\rm f}$) along the channel direction y [2]

$$j_{\rm n} = -q\mu n \frac{d\phi_{\rm f}}{dy}.$$

This leads to the drain current ($I_{\rm ds}$) equation as a function the drain voltage ($V_{\rm ds}$) as

$$I_{\rm ds} = qW_{\rm ch}\mu n_{\rm av}\frac{V_{\rm ds}}{L_{\rm ch}} = qW_{\rm ch}\mu\frac{V_{\rm ds}/L_{\rm ch}}{\left(\int_0^{L_{\rm ch}} n_{\rm x}^{-1}dy\right)/L_{\rm ch}} \qquad (1)$$

where n_x is the integrated concentration along the depth direction. The inverse of the denominator of the right-hand side equation is defined as n_{av}. Parameters q, L_{ch}, W_{ch} and μ are the electron charge, the channel length, the channel width, and the electron mobility, respectively.

The pocket profile is modeled by a linearly graded function along the channel with the parameters L_p and N_{subp} as depicted in Fig. 2. The bulk concentration is homogeneous and fixed to N_{subc}.

Fig. 3 shows simulated carrier concentrations vs. V_{gs} with MEDICI for different channel concentrations, where n_c and n_p are homogeneous cases with $N_{subc}(< N_{subp})$ and $N_{subc}(= N_{subp})$, respectively. As can be seen, different N_{sub} concentrations lead to different V_{gs} at which the threshold condition is fullfilled. In the technology studied here, N_{subc} and n_{th} are $5 \times 10^{17} cm^{-3}$ and $1.5 \times 10^{10} cm^{-2}$, respectively. For analytical description of n_{av} we propose the equation

$$n_{av} = A n_c \tag{2}$$

with

$$A = L_{ch}/(L_{ch} + 2L_p(n_c/n_p - 1)) \leq 1$$

Eq. (2) means that $n_{c,th}$ must become larger than n_{th} at the threshold condition to preserve $n_{av,th} = n_{th}$ for the pocket-implant case, as schematically depicted in Fig. 3. Consequently $n_{c,th}$, the carrier concentration of the non-pocket channel region at V_{th}, varies with the pocket profile parameters and channel length. If L_p and N_{subp} are given, n_c and the ratio n_c/n_p in eq. (2) can be calculated by solving the Poisson equation. The final analytical V_{th}-description is

$$V_{th(pocket)} = \phi_{th} + V_{fb} + \frac{\sqrt{2qN_{subc}\epsilon_{si}(\phi_{th} - V_{bs})}}{C_{ox}} \tag{3}$$

where the threshold surface potential ϕ_{th}, giving the $n_{c,th}$ value in eq. (2), is obtained by solving the Poisson equation under the Gauss law.

Though all descriptions are given for the n-channel case, they are valid for the p-channel case as well.

3 Results and discussion

The derivation of eqs. (1)-(3) assumes a small V_{ds} ($\leq 50mV$). When V_{ds} increases, a surface potential increase occurs only in the drain-side pocket for long-channel cases as demonstrated in Fig. 4.

Fig. 5a shows the subthreshold characteristics simulated with MEDICI for different channel conditions and V_{ds} values. With only a drain-side pocket an enhanced SCE is observed, which can be modeled by a reduced gate-length to pocket-penetration length L_p and a linear increasing channel concentration added in the conventional V_{th}-model [3]. With only a source-side pocket the V_{th} dependence on V_{ds} due to the SCE is totally suppressed as can be seen in Fig. 5b. With pockets on both sides an averaged V_{th} dependence on V_{ds} is observed. Therefore the SCE is present in pocket-implant MOSFETs up to the long-channel range, preventing the desirable voltage saturation for large V_{ds}.

Calculated $V_{th} - L_{gate}$ characteristics are depicted by solid lines in Fig. 1. Fig. 2 also shows the pocket-profile obtained from TSUPREM by inverse modeling. The

model profile is about the average of the real pocket profile along the vertical direction. Though the simple linearly-graded model profile shows deviations from reality for extremely short $L_{\rm gate}$, agreement is in general good as demonstrated in Fig. 6. For $L_{\rm gate} \leq 0.3\mu m$, the pockets from the source side and the drain side overlap, and the channel concentration eventually becomes even higher than $N_{\rm subp}$. This is also included in our model by adding two pocket concentrations according to the strength of their overlap.

The model describes the lateral distribution of the pocket profile as shown in Fig. 2. However, the vertical profile plays also a role for the $V_{\rm th}$ characteristics. The vertical profile can be determined in addition by adjusting measured $V_{\rm th}$ *vs.* $\sqrt{\phi_{\rm th} - V_{\rm bs}}$ characteristics as demonstrated in Fig. 7 [4]. For reduced $L_{\rm gate}$, deviation of calculated $V_{\rm th}$ *vs.* $\sqrt{\phi_{\rm th} - V_{\rm bs}}$ becomes obvious. The reason is the impurity-concentration increase of the pocket profile in the direction vertical to the channel. We use this deviation to extract the vertical profile for obtaining an accurate impurity concentration below the gate oxide, which is important for the on-current characteristics.

4 Conclusion

We have developed a new $V_{\rm th}$ model for both circuit simulation and pocket-profile optimization. The basic idea is to introduce an average carrier concentration to determine $V_{\rm th}$. This concentration is well defined by the maximum concentration of the pocket and its penetration length into the channel. The model reproduces measured $V_{\rm th}$ within an accuracy of a few mV.

References

[1] Y. Taur and E. J. Nowak, IEDM Tech. Dig. p215, 1997.
[2] S. Sze, "Physics of Semiconductor Device", Wiley, 1981.
[3] M. Miura-Mattausch et al., IEEE Trans. CAD/ICAS, vol. 15, 1, 1996.
[4] M. Suetake et al., Proc. SISPAD, p207, 1999.

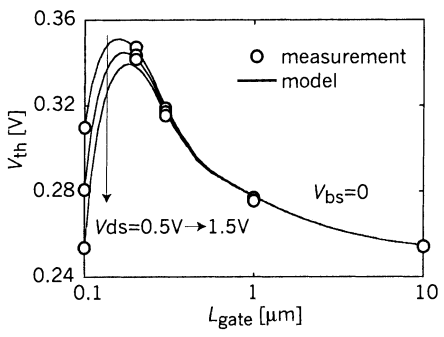

Fig. 1. $V_{\rm th}$ vs. $L_{\rm gate}$ for a pocket implant technology. Symbols are measurements and solid lines are model results.

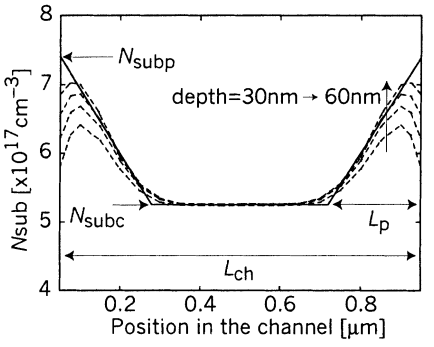

Fig. 2. Extracted pocket-profile model depicted by a thick solid line. The dashed curves are TSUPREM results for various depths.

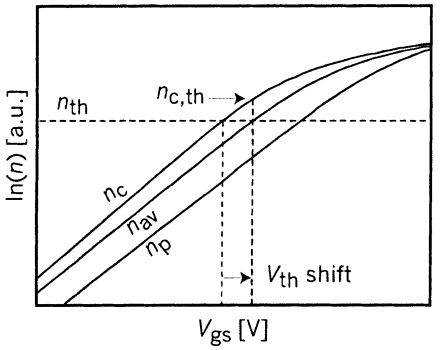

Fig. 3. Simulated carrier concentrations as a function of the gate voltage V_{gs} for two homogeneous substrate concentrations without pocket implantation (n_c and n_p) and with the pocket (n_{av}).

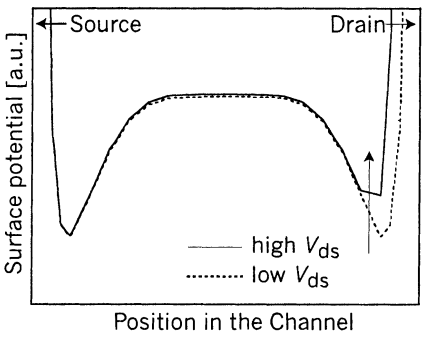

Fig. 4. Simulated surface potential distribution along the channel for two V_{ds} values.

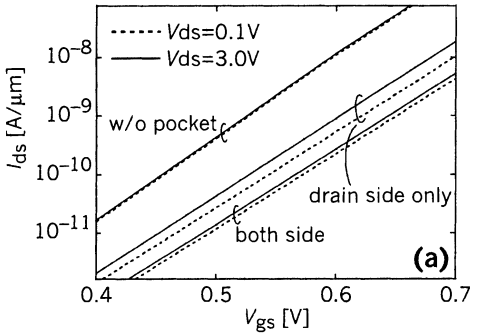

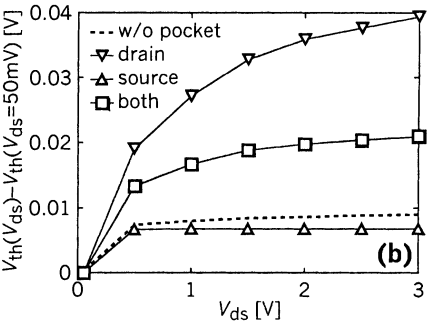

Fig. 5. (a) Simulated I-V characteristics of $L_{gate} = 1.0\mu m$ with MEDICI for different substrate conditions, without the pocket implantation, the pocket only at the drain side, and at the both sides. (b) Simulated V_{th} shift from V_{th} at $V_{ds} = 50mV$ as a function of the drain voltage V_{ds}.

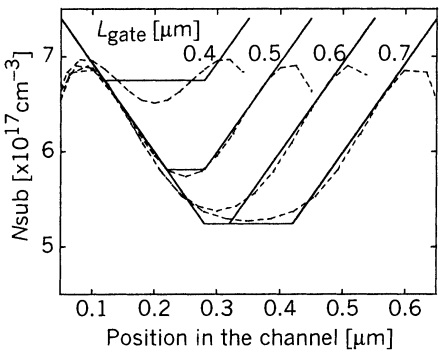

Fig. 6. Extracted pocket profile along the channel for different L_{gate} lengths (solid line). Dashed curves are results with TSUPREM at the depth of 50nm.

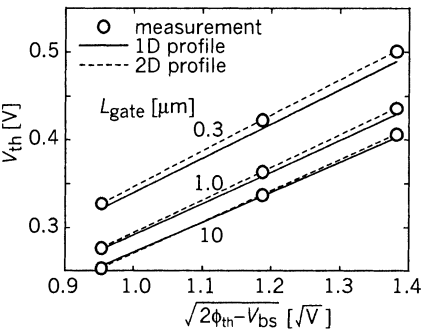

Fig. 7. Comparison of calculated V_{th} body coefficients. Symbols are measurements and thick solid lines are results with the pocket-profile model shown in Fig. 6. Dashed lines are results with the 2D pocket profile including the gradient to the depth direction.